Electropolymerization Studies on a Series of Thiophene-Substituted 1,3-Dithiole-2-ones: Solid-State Preparation of a Novel TTF-Derivatized Polythiophene

Tania Anjos,[†] Adam Charlton,[†] Simon J. Coles,[‡] Anna K. Croft,[†] Michael B. Hursthouse,[‡] Maher Kalaji,[†] Patrick J. Murphy,*[,†] and Susan J. Roberts-Bleming[†]

School of Chemistry, Bangor University, Bangor, Gwynedd LL57 2UW, U.K., and School of Chemistry, University of Southampton, Southampton SO17 1BJ, U.K.

Received September 30, 2008; Revised Manuscript Received January 16, 2009

ABSTRACT: The synthesis, electrochemical and spectroscopic properties of a series of thiophene-substituted 1,3-dithiole-2-ones is described. The derivatives **Th-3,3**, **Th-2,2**, **Th-2,3**, **Th-3,3(2,2′-Me)**, and **Th3,3-(2,5,2′,5′-Me)**, have been successfully polymerized by cyclic voltammetry. From the UV−visible spectra of the neutral films, it was determined that **PTh-3,3**, **PTh-2,2** and **PTh-2,3** have a bandgap of 2.04, 2.30, and 2.18 eV, respectively. The voltammetric response of **Th-3,3(2,2′-Me)** was noticeably different from the other polymers. The SNIFTIRS data suggested that **Th-3,3(2,2′-Me)** was formed by bonding via the β-positions of the thiophene ring, resulting in a poorly conductive polymer. The in situ solid-state modification of **PTh-3,3** to produce a new TTF-derivatized polythiophene was carried out. The cyclic voltammetry of the modified polymer confirmed the inclusion of TTF into the backbone of the film.

Introduction

The prospect of using conducting polymers in biosensors,[1] molecular electronics,[2] electrochromic displays,[3] solar cells,[4] or electrochemical storage systems,[5] among other possibilities, has increased the interest of researchers in this important field.[6] In the search for commercially viable conducting polymers, polythiophenes have been widely studied because they are electroactive materials with high environmental and thermal stability.[7,8] They also exhibit high electrical conductivities in the doped state, which results from the highly conjugated, structurally regular nature of the polymer backbone.[9] The vast volume of research undertaken on polythiophenes has led to their many applications, e.g., in electrochromic devices,[10,11] polymer light-emitting diodes,[12] sensors,[13] and batteries.[5] In the present work, we report on the synthesis and study of the physical properties of a series of thiophene-substituted 1,3-dithiole-2-ones (Figure 1).

Apart from the preparation and study of new polythiophenes, a great deal of effort has been directed toward modifying existing conducting polymers to improve desirable properties such as solubility, stability, strength, and conductivity.[14] One approach that is receiving increasing attention is functionalization after polymerization, for example, the incorporation of groups, such as tetrathiafulvalene (TTF) into the polymer backbone. This process can give access to polymers that cannot be directly obtained by electropolymerization of the corresponding monomers, either because substituent groups were sensitive to the oxidative conditions of film growth, or because they inhibited the polymerization process.[15]

The first report of an electropolymerized TTF-derivatized polythiophene was published in 1991 by Bryce and coworkers,[16] describing the formation of a polymer film based on a thiophene unit linked to the TTF redox active center via an ester group linkage. This polymer was found to have short conjugation length, which was probably due to distortion in the PT backbone

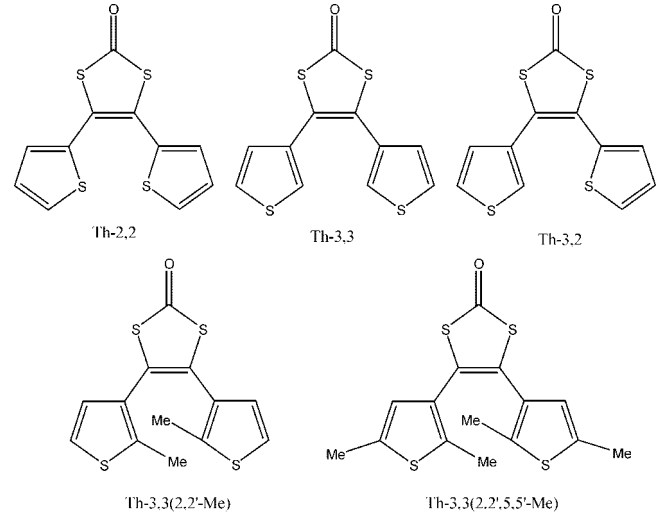

Figure 1. Structures of 4,5-*bis*-thiophen-3-yl-[1,3]dithiol-2-one (**Th-3,3**), 4-thiophen-3-yl-5-thiophen-2-yl [1,3]dithiol-2-one (**Th-2,3**), 4,5-*bis*-thiophen-2-yl-[1,3]dithiol-2-one (**Th-2,2**), 4,5-*bis*-(5-methyl-thiophen-3-yl)-[1,3]dithiol-2-one (**Th-3,3(2,2′-Me)**), and 4,5-*bis*-(2,5-dimethyl-thiophen-3-yl)-[1,3]dithiol-2-one (**Th-3,3(2,2′5,5′-Me)**).

produced by the steric interactions between pendant TTF groups.[17] Subsequent to this, a wide range of polythiophenes linked to TTF units via saturated spacer groups have been synthesized.[17−19] Even though the design of these polymers provides for the close spatial proximity of the redox centers, they cannot ensure a well-defined orientation of the TTF groups relative to one another because the torsion around the bridging bonds allows for a number of different conformations.

The electropolymerization of TTF−thiophene monomers in which these two redox-active moieties are directly bonded to each other is still seen to be a rather difficult process.[20] For instance, Charlton et al.[21,22] produced a series of new thiophene-functionalized TTF derivatives that could not be polymerized because of disruption in the aromaticity of the dicationic TTF core, generated in solution prior to the oxidation of the thiophene

* Corresponding author. E-mail: chs027@bangor.ac.uk.
[†] University of Bangor.
[‡] University of Southampton.

10.1021/ma802181b CCC: $40.75
Published on Web 03/10/2009

Scheme 1. In Situ Modification of Polythiophene 1,3-Dithiole-2-ones at an Electrode Surface[a]

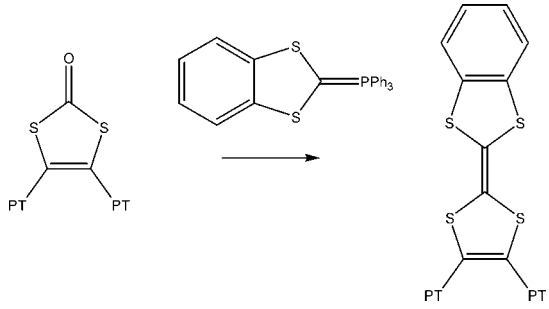

[a] PT = polythiophene chain.

Scheme 2. Preparation of Th-3,3, Th2,2, Th-3,3(2,2′-Me), and Th-3,3(2,2′,5.5′-Me)[a]

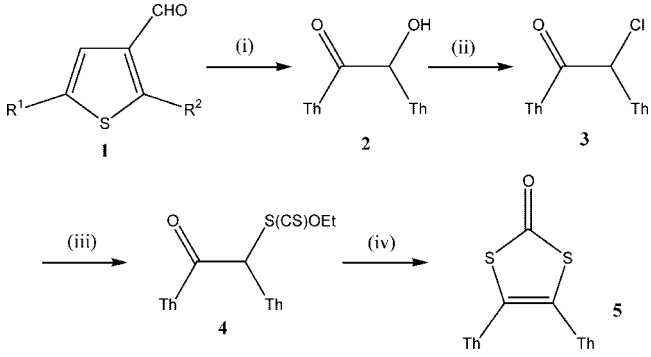

[a] Reagents and conditions: (i) 3-Benzyl-5-(2-hydroxymethyl)-4-methyl-1,3-thiazolium chloride, NEt_3/EtOH; (ii) PPh_3, CCl_4/CH_2Cl_2, RT; (iii) KSC(S)OEt, acetone, RT; (iv) HBr, AcOH. R^1, R^2 = H, Me.

units. To avoid the problematic polymerization of the TTF-derivatized thiophene monomers, the in situ solid-state modification of polymerized thiophene-substituted 1,3-dithiole-2-ones using Wittig methodology was investigated. (Scheme 1).

Results and Discussion

The synthesis of the monomeric starting materials **Th-3,3**,[23] **Th-2,2**,[21,24] **Th-3,3(2,2′-Me)**, and **Th-3,3(2,2′,5.5′-Me)** is shown in Scheme 2. The first step in the synthesis of the three substituted 1,3-dithiol-2-ones involves the benzoin condensation of the requisite aldehyde **1** to give the α-hydroxy ketone **2**. Reaction of **2** with triphenylphosphine and carbon tetrachloride leads to the chloride **3**, which is immediately converted to the more stable xanthate **4** by reaction with potassium ethyl xanthate in acetone. Cyclization of **4** is achieved by treatment with HBr in acetic acid, resulting in the formation of the required monomers **Th-2,2**,[23] **Th-3,3**,[21,24] **Th-3,3(2,2′-Me)**, and **Th-3,3(2,2′,5.5′-Me) 5**. The structures of **Th-3,3**, **Th-3,3(2,2′-Me)**, and **Th-3,3(2,2′,5.5′-Me)** were confirmed by X-ray analysis. (See the Supporting Information.)

4,5-Bis-(5-methyl-thiophen-3-yl)-[1,3]dithiol-2-one Th-3,3(2,2′-Me). 2-Methyl-3-thiophene carboxaldehyde[25] (8.3 g, 65.9 mmol) was dissolved in absolute ethanol (200 mL), whereupon triethylamine (2.0 g, 20 mmol) and 3-benyl-5-(2-hydroxyethyl)-4-methylthiazolium chloride (3.6 g, 10 mmol) were added, and the mixture was refluxed for 5 h. After cooling, water (200 mL) was added, and the reaction extracted dichloromethane (3 × 100 mL). The combined organic fractions were washed with brine (75 mL), dried ($MgSO_4$), and evaporated. The crude product was purified using silica gel chromatography eluting (diethyl ether/petroleum ether 10:90 and 20:80) to give 2-hydroxy-1,2-bis-(2-methyl-thiophen-3-yl)-ethanone (2.3 g, 9.1 mmol, 28%). R_f 0.68 (20:80 diethyl ether/petrol). mp 83−86 °C. δ_H 6.9 (d, 2H, *J* 5.5 Hz, CH), 6.9 (d, 1H, *J* 5.5 Hz, CH), 6.6 (d, 1H, *J* 5.3 Hz, CH), 5.6 (d, 1H, *J* 5.4 Hz, CH), 4.5 (d, 1H, *J* 5.4 Hz, OH), 2.7 (s, 3H, CH_3), 2.5 (s, 3H, CH_3). δ_C 194.3, 152.4, 137.7, 134.8, 131.8, 127.4, 126.7, 122.7, 121.8, 71.1, 16.3, 13.1. ν_{max} 2921 (C−H), 1666 (C═O), 1508 (C═C). HRMS $C_{12}H_{16}S_2NO_2$ [M + NH_4]: required, 270.0622; found, 270.0620.

The α-hydroxyketone (2.2 g, 8.7 mmol) was dissolved in dichloromethane (10 mL) and added to a solution of triphenylphosphine (4.6 g, 17.5 mmol) in CCl_4 (30 mL), and the mixture was stirred in the dark for 18 h. The reaction was poured onto a prewashed (with CCl_4) column of silica gel (150 g) and eluted with diethyl ether/petrol (50:50) to give the desired chloride (1.9 g, 7.0 mmol, 81%) as a waxy yellow solid that was used immediately in the next step. The chloride (1.9 g, 7.0 mmol) was dissolved in acetone (10 mL) and added to a stirred solution of potassium ethyl xanthate (1.11 g, 7.0 mmol) in acetone (70 mL), and the mixture was stirred for 15 min. Diethyl ether (200 mL) was added, and the resulting precipitate was removed by filtration through a pad of silica gel. The filtrate was evaporated to give the xanthate (2.5 g, 7.0 mmol, 100%) as an off-white solid. The xanthate (2.5 g, 7.0 mmol) was dissolved in glacial acetic acid (15 mL); 45% hydrobromic in acetic acid (15 mL) was then added, and the mixture was stirred vigorously for 15 min. Dichloromethane (50 mL) and water (200 mL) were added, the resultant mixture was separated, and the aqueous phase was extracted with additional dichloromethane (3 × 25 mL). The combined organic fractions were washed with sodium bicarbonate solution (sat. 3 × 25 mL), dried ($MgSO_4$), and evaporated in vacuo. The crude product was purified by silica gel chromatography eluting with diethyl ether/petroleum ether (3:97, 10:90, 30:70), followed by recrystallization from hexane/diethyl ether to give **Th-3,3(2,2′-Me)** (1.1 g, 3.5 mmol, 51%) as pale-yellow needles. mp 131−135 °C. δ_H 7.0 (d, 1H, *J* 5.1 Hz, CH), 6.8 (d, 1H, *J* 5.5 Hz, CH), δ 2.1 (s, 6H); δ_C 191.1, 142.6, 128.4, 126.1, 124.9, 122.6, 13.9. ν_{max} 2920 (C−H), 1653 (C═O), 1545 (C═C). HRMS $C_{13}H_{14}NOS_4$ [M+NH_4^+]: required, 327.9958; found, 327.9957.

4,5-Bis-(2,5-dimethyl-thiophen-3-yl)-[1,3]dithiol-2-one (Th-3,3(2,2′,5.5′-Me). 2,5-Dimethylthiophene carboxaldehyde[26] (4.9 g, 35.0 mmol) was dissolved in isopropanol (9.4 mL) together with triethylamine (1.1 g, 11.0 mmol) and 3-benzyl-5-(2-hydroxyethyl)-4-methyl-1,3-thiazolium chloride (5.8 g, 21.0 mmol), and the mixture was heated at reflux for 48 h. Water (150 mL) was added, and the mixture was extracted with DCM (3 × 30 mL). The combined organic residues were washed with $NaHCO_3$ (sat. 30 mL), dried ($MgSO_4$), and evaporated in vacuo, producing a brown solid that was purified by silica gel chromatography eluting with diethyl ether/petrol (30:70) to give 1,2-bis-(2,5-dimethyl-thiophen-3-yl)-2-hydroxy-ethanone (0.76 g, 2.71 mmol, 16%). R_f 0.15 (20:80 diethyl ether/petrol). mp 144−146 °C. δ_H 6.8 (s, 1H, CH), 6.3 (s, 1H, CH), 5.5 (d, 1H, *J* 5.5 Hz CH) 4.4 (s, 1H, *J* 5.5 Hz OH), 2.7 (s, 3H, CH_3), 2.5 (s, 3H, CH_3) 2.3 (s, 6H, 2 × CH_3). δ_C 194.2, 150.7, 136.9, 135.6, 135.1, 134.4, 131.6, 124.9, 124.2, 70.9, 16.3, 15.1, 15.0, 13.0. ν_{max} 3097 (O−H), 2918 (C−H), 1659 (C═O), 1550 (C═C). HRMS $C_{14}H_{16}S_2O_2$: required, 280.0592; found, 280.0592.

The α-hydroxyketone (2.2 g, 7.86 mmol) was dissolved in dichloromethane (30 mL), a solution of triphenylphosphine (4.6 g, 17.5 mmol) in CCl_4 (10 mL) was added, and the resultant solution was stirred in the dark for 18 h. The crude reaction mixture was poured onto a silica gel column (150 g, preloaded with CCl_4) and eluted with 50:50 diethyl ether/petrol. Fractions containing the product (R_f = 0.32 in 50:50 diethyl ether/petrol) were combined and evaporated to give the chloride (1.9 g, 7.86 mmol, 81%). The chloride (0.6 g, 2.0 mmol) was dissolved in

Scheme 3[a]

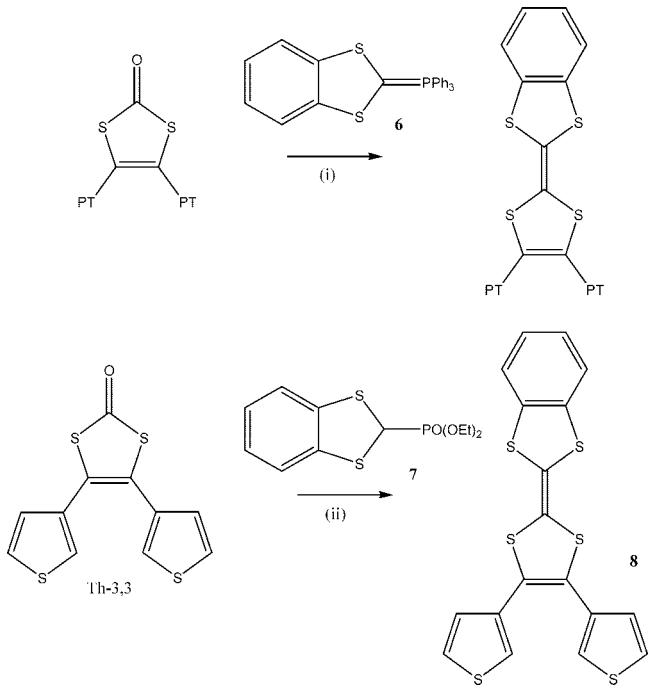

[a] Reagents and conditions: (i) dry Et_2O, *n*-BuLi, 0 °C. (ii) *n*-BuLi, −78 °C, rt 1 h, 54%.

dry acetone (50 mL), a solution of potassium ethyl xanthate (0.5 g, 3.1 mmol) in acetone (20 mL) was added, and the mixture was stirred for 30 min. Diethyl ether (80 mL) was added, and the resulting precipitate was removed by filtration through a silica pad. Evaporation of the filtrate gave the xanthate (0.6 g, 1.65 mmol, 78%) as a cream-colored solid that was immediately used in the next step of the reaction. The xanthate (0.6 g, 1.65 mmol) was dissolved in glacial acetic acid (5 mL), hydrobromic acid (5 mL, 45% w/v) was added, and the mixture was vigorously stirred for 15 min. Water (50 mL) and dichloromethane (50 mL) were added, the organic layer separated, and the aqueous phase was extracted with further dichloromethane (3 × 25 mL). The combined organic fractions were washed with $NaHCO_3$ solution (sat. 3 × 20 mL), dried ($MgSO_4$), and evaporated in vacuo. Silica gel chromatography (diethyl ether/petrol, 3:97 and 10:90) gave **Th-3,3(2,2′,5.5′-Me)** (0.3 g, 0.8 mmol, 54%). mp 295−298 °C. δ_H 6.4 (s, 2H, CH), 2.3 (s, 6H, 2 x CH_3), 2.0 (s, 6H, 2 × CH_3). δ_C 191.4, 136.6, 132.6, 128.6, 127.6, 124.8, 32.2, 29.6. ν_{max} 2920 (C−H), 1670 (C═O), 1545 (C═C). HRMS $C_{15}H_{12}S_4O$ [M^+]: required, 337.9927; found, 337.9913.

Following the electrochemical growth of **PTh-2,3**, **PTh-3,3**, and **PTh-2,2** films, their modification to the TTF derivatives (Scheme 1) was attempted. The modification was performed under Wittig conditions with the ylid **6**[27] generated in situ in diethyl ether, which was found to react with the polymeric film deposited on the electrode. Initial attempts were made to react the films with the phosphonate **7**[28] under Wadsworth−Emmons conditions; however, the solvent required for this (THF) was found to destroy the deposited films after exposure for a short time. Interestingly, the lithiated phosphonate reacts with the monomeric **Th-3,3** to give the TTF **8**, the structure of which was confirmed by X-ray crystallography (Scheme 3). (See the Supporting Information).

2-(4,5-Dithiophen-3-yl-[1,3]dithiol-2-ylidene)-benzo[1,3]dithiole 8. *n*-BuLi (2.5 M in hexanes, 1.38 mL, 3.5 mmol) was added to a stirred, cooled (−78 °C) solution of **7** (1.0 g, 3.45 mmol) in THF (15 mL). After 15 min, **Th-3,3** (0.2 g, 0.67 mmol) dissolved in THF (10 mL) was added, and the reaction was stirred at this temperature for 20 min and then slowly warmed to rt and stirred for 1 h. The reaction mixture was evaporated in vacuo, and dichloromethane (50 mL) and HCl (50 mL) were added. The organic layer was separated, and the aqueous layer was extracted with further dichloromethane (3 × 50 mL). The combined organic extracts were washed with H_2O (25 mL), dried ($MgSO_4$), and evaporated. Purification by silica gel chromatography (0:100, 5:95, 10:90 diethyl ether/petrol) gave **8** (0.15 g, 0.36 mmol, 54%) as dark-orange crystals from hexane/diethyl ether (3:1). R_f 0.64 (5:95 diethyl ether/petrol). mp 101−104 °C. δ_H 7.3 (m, 4H, 4 × CH), 7.1 (m, 4H, 4 × CH), 6.9 (d, 2H, *J* 4.4 Hz, 2 × C−H). ν_{max} 1657 (C═C), 3111 (C−H), 3098 (C−H). HRMS $C_{18}H_{10}S_6$: required, 417.9107; found, 417.9109.

Compound **8** was analyzed by cyclic voltammetry in a 0.1 M solution of TBATFB/MeCN showing a behavior typical of TTF derivatives in which the characteristic TTF redox couples appeared at E_{ox}^1 + 0.68 V and E_{ox}^2 + 1.07 V versus Ag wire. These values are, as expected, shifted toward more positive potentials compared with TTF itself.

Computational, Electrochemical, and Spectroelectrochemical Studies. *Experimental Section.* Gaussian B3LYP energy calculations[29] were done on **Th-3,3**, **Th2,2**, **Th-2,3**, and **Th-3,3(2,2′-Me)**. The B3LYP/6-31G(d) electronic energies of each compound were calculated using the optimized structures. Vertical ionization energies were calculated using the optimized structure of the radical cations.

The electrochemistry of **Th-3,3**, **Th-2,2**, **Th-2,3**, and **Th-3,3(2,2′-Me)** was investigated by cyclic voltammetry using an electrolyte solution containing monomer units (0.01 M). The electrolyte was made up of tetra-*n*-butyl ammonium hexafluorophosphate ($TBAPF_6$ purity >98%, Avocado Research Chemicals; 0.1 mol dm^{-3}) in acetonitrile (CH_3CN purity >99.9%, Riedel-de Häen; stored over molecular sieves). A silver wire immersed in a solution of $AgNO_3$ (0.01 M) in the same electrolyte solution was the reference electrode (+0.32 V vs SCE). The experiments were performed in a three-electrode glass cell using a platinum disk as the working electrode (electrode area = 0.44 cm^2), a platinum foil as the counter electrode, and Ag/Ag^+ as the reference electrode. All potentials values presented in this report are quoted against the SCE. Attempts to grow the polymeric films were carried out potentiodynamically by cycling the electrode potential in an electrolyte solution containing the monomer units. All voltammetry experiments were carried out using a potentiostat, and a waveform generator (HI-TEK instruments PP R1). The output was plotted using an X−Y recorder (LLOYD instruments PL3).

Subtractively normalized interfacial Fourier transform infrared spectroscopy (SNIFTIRS) measurements were performed using a completely evacuated Bruker IFS 113v computer-controlled FT-IR spectrometer. The optics bench was evacuated prior to any experiment to eliminate interference from atmospheric CO_2 and H_2O. The spectrometer operates with a silicon carbide source, which has a range of 6000−100 cm^{-1}, an MCT (mercury−cadmium−telluride) liquid-nitrogen-cooled detector, and a Ge/KBr beam splitter. A silicon disk was used as the infrared transparent window, separating the electrochemical cell from the evacuated spectrometer. The instrument was setup to allow external reflection by focusing the IR beam onto the working electrode. The potential was applied to the working electrode using a potentiostat, HI TEK type DT2101, connected to a waveform generator (HI-TEK instruments PP R1). The electrode potential was then allowed to stabilize before the IR data were collected. The difference spectra were obtained by subtracting two spectra (S2 and S1) collected at different potentials (E_2 and E_1, respectively) and dividing by the spectrum

Table 1. Calculated Vertical Ionization Energies for Th-3,3, Th-2,2, and Th-2,3

	(i) optimized B3LYP energy (eV)	(ii) radical cation B3LYP energy (eV)	Δ(i)/(ii) (eV)
Th-3,3	56 892.21	56 884.94	7.264
Th-2,2	56 892.14	56 885.08	7.065
Th-2,3	56 892.19	56 885.02	7.165

obtained at E_1 (S1). The positive and negative bands in the normalized difference spectra indicate decreased and increased absorbances, respectively, at E_2. Throughout these studies, 100 interferograms were collected at each potential. Because no logarithm was applied, the difference spectra are shown as reflectance units ($\Delta R/R$).

Computational Studies of Thiophene-Substituted 1,3-Dithiole-2-ones. The optimized gas-phase minimum energy structure was calculated for each 1,3-dithiole-2-one and respective radical cation. The vertical ionization potentials (IPs) were calculated by subtracting the absolute energy of the radical cation from the absolute energy of the neutral compound (Table 1).

The results shown in Table 1 suggest that **Th-2,2**, having the lowest vertical ionization energy, is expected to be easier to oxidize than all of the other substrates. On the contrary, **Th-3,3** is predicted to have a high oxidation potential.

Electrochemical and Spectroelectrochemical Studies on **Th-3,3**. A solution of **Th-3,3** was analyzed by cyclic voltammetry; polymerization was successfully achieved by cycling the electrode potential between 0.8 and 1.7 V, as shown in the Figure 2a.

The growth of the polymer is typical of that of other conducting polymers, and Figure 2b shows the voltammetric response obtained between 0.3 and 1.35 V. Polymer oxidation occurs when the potential is taken from 1.08 to 1.35 V. A clear reduction peak can then be seen in the reverse scan at 1.22 V. The film was cycled repeatedly between −1.5 and 2.1 V without any significant loss of electroactivity. The switching of **PTh-3,3** between the neutral and oxidized state was accompanied by a reversible color change from yellow (neutral polymer) to black (oxidized polymer). The reversible change in color of polythiophenes upon electrochemical doping has been well documented.[30−32] Whereas in the neutral state, the color is determined by the band gap of the polymer, as electrons are added or removed (doping), new electronic states are formed in the band gap, giving rise to optical absorption at energies lower than the original band gap.[33]

SNIFTIRS studies were carried out to investigate the changes in the IR spectra of **PTh-3,3** upon doping. To facilitate the assignment of the IR absorption peaks present in the SNIFTIR spectra, an IR spectrum of the monomer **Th-3,3** was initially recorded. In the FTIR spectrum of monomeric **Th-3,3**, peaks at 3103 and 3081 cm^{-1} can be assigned to the C_α-H and C_β-H stretching vibrations, respectively.[34,35] The C−S asymmetric and symmetric stretching vibrations can be found at 859 and 841 cm^{-1}.[36,37] A strong peak arising from the C═O stretching is seen at 1630 cm^{-1}.[38] Smaller bands at 1571 and 1481 cm^{-1} are assigned to the C═C ring vibration.[39] Peaks at 703 and 784 are due to the out-of-plane deformation of the C_α-H and C_β-H bonds, correspondingly.[40,41]

Figure 3 shows the SNIFTIR spectra of **PTh-3,3** collected at successively higher potentials and normalized to the reference spectrum taken at 0.3 V. Upon oxidation, new IR vibrations can be seen at 1298, 1190, 1156, and 1013 cm^{-1}. These bands (IRAV: infrared active vibrations) appear at about the same position in the FTIR spectra of doped PT and are due to the selective enhancement of four thiophene ring modes caused by the coupling of the movement of charge carriers with the polymer lattice vibrations.[7,42−44] In addition, the shape and position of the IRAV bands are not changed upon p-doping, indicating that the same type of charge carriers are responsible for the conduction in the potential range studied. The spectra of **PTh-3,3** also reveal a very broad absorbance extending from about 1950 cm^{-1} (0.24 eV) into the Near IR. This band is believed to be due to the electronic transition between the valence band and the lowest polaron or bipolaron state.[45,46]

The incorporation of anions, the main charge compensation process during the oxidation of polythiophenes, can be observed as an increasing negative band related to the insertion into the film of PF_6^- (anion present in the electrolyte) at 839 cm^{-1}.[47,48] Other electrolyte bands are seen pointing upward at 2250 cm^{-1} (acetonitrile C≡N stretch) and centered at 3000 cm^{-1} (TBA^+).[37]

The absence of the C_α-H stretching vibration peak at 3103 cm^{-1} indicates that the coupling of thiophene units mainly takes place through the α-positions. It can also suggest the occurrence of intramolecular cyclization during the polymerization process due to the proximity of the C_α-H bonds in the thiophene rings of each monomer molecule. Taking this into account, a possible structure of **PTh-3,3** is shown in Figure 4.

In the SNIFTIRS spectra of **PTh-3,3**, low intensity bands appearing at 1524, 1363, and 939/855 cm^{-1} can be assigned to the stretching vibrations of C═C, C−C, and C−S, correspondingly.[37,47,49] Another important region to highlight is that around 1700 cm^{-1}. This spectral region is especially informative about the effect of the doping process on the strength of the C═O bond. This bond is affected by the electronic changes within the polymer backbone, as reported by Beyer et al.[48] Upon p-doping the positive charge on the carbonyl carbon atom increases, which creates a polarized bond resulting in increased bond strength. This will be manifested by a shift in the carbonyl group frequency to a higher wavenumber (blue shift). Experimental evidence of this phenomenon is indeed observed upon p-doping, with the peak corresponding to the neutral carbonyl group at 1664 cm^{-1} being gradually lost (positive band) and the peak associated with the oxidized polymer at 1710 cm^{-1} becoming increasingly dominant (negative band).

UV−visible spectroscopy has been used to examine the optical behavior **PTh-3,3** upon doping. In situ spectroelectrochemical measurements were performed in a monomer-free electrolyte solution using the same range of potentials as those applied during the characterization of the film by voltammetry. A series of UV−visible spectra were taken at successively higher doping levels. Figure 5 shows the in situ absorbance spectra recorded for a **PTh-3,3** film grown on ITO.

Neutral **PTh-3,3** exhibits an absorption maximum centered at 410 nm that can be assigned to the π-π^* transition.[50] The electronic bandgap of the polymer, defined as the onset for the π-π^* absorbance, is approximately 2.04 eV. The oxidation of **PTh-3,3** is characterized by the emergence of a new band at λ_{max} = 655 nm (onset at 1.64 eV) corresponding to the formation of the (bi)polaronic state.[51] An isosbestic point is observed around 525 nm, implying the coexistence of two regions in doped **PTh-3,3**: a neutral region where the π-π^* transition is unchanged and localized regions surrounding the charge storage configuration (fully doped polymeric chains).[52−55]

Using SNIFTIRS, a second subgap electronic transition has been previously identified at 0.24 eV (Figure 5); therefore, two electronic transitions took place below the bandgap energy level upon electrochemical oxidation. It has been recognized that the formation of the bipolaronic and polaronic states leads to two and three subgap electronic transitions, respectively.[56,57] Therefore, because **PTh-3,3** displays only two new optical transitions upon doping, it can be assumed that bipolarons are

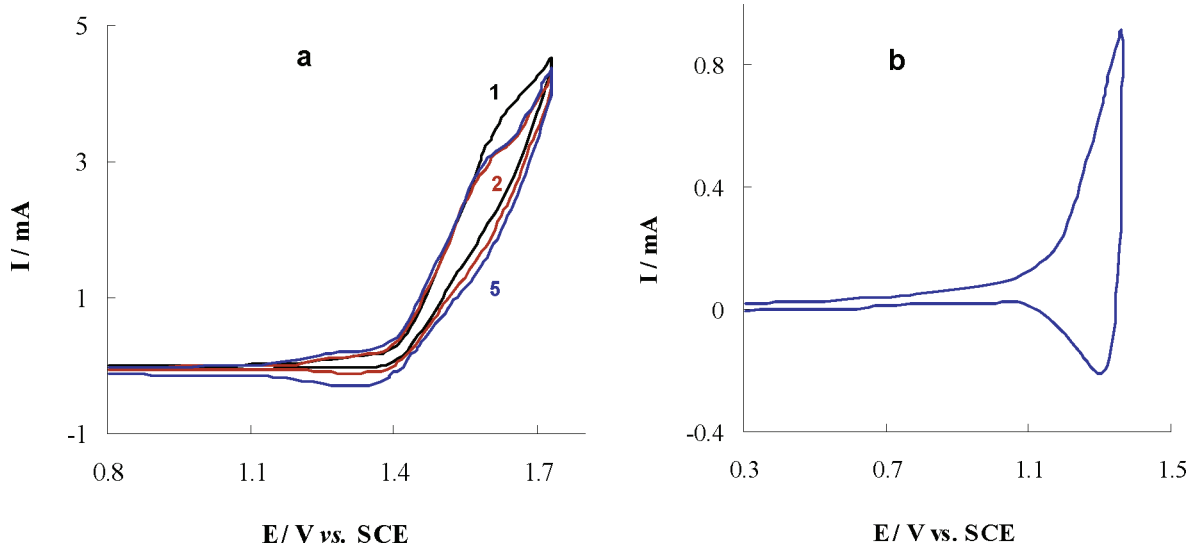

Figure 2. (a) Voltammograms of the polymerization of **Th-3,3** recorded at 0.1 V s^{-1} (1st, 2nd, and 5th cycles) and (b) cyclic voltammogram of **PTh-3,3** in monomer-free solution recorded at $v = 0.1$ V s^{-1} using a Pt disk working electrode (0.44 cm^2).

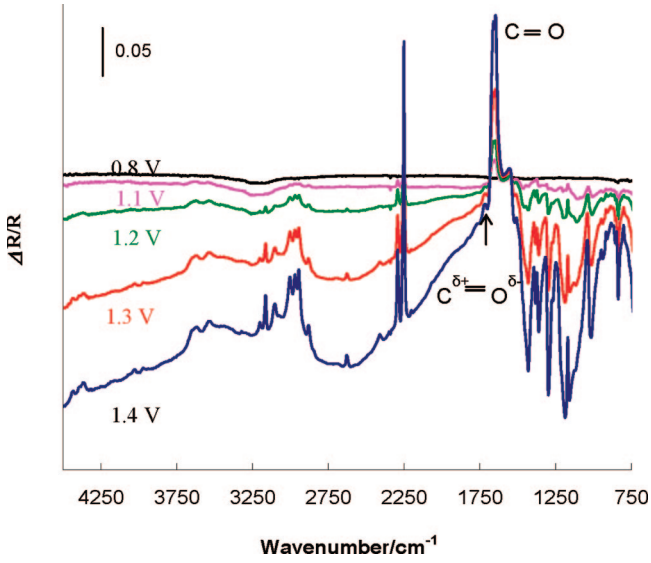

Figure 3. SNIFTIRS spectra of **PTh-3,3** taken from 0.8 to 1.4 V. Reference spectra collected at 0.3 V.

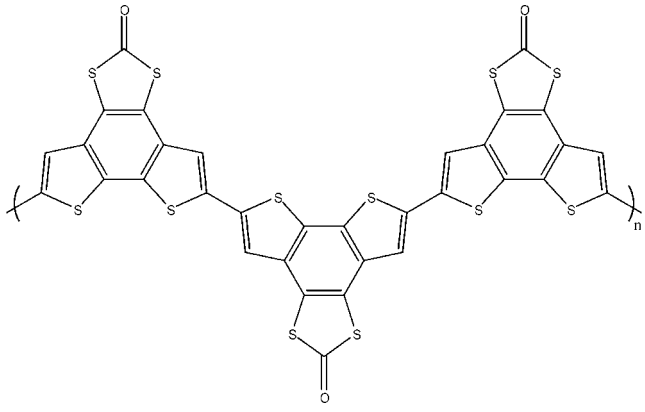

Figure 4. Proposed structure for **PTh-3,3**.

most likely the charge carriers, as shown in the energy level diagram of Figure 6

Electrochemical and Spectroelectrochemical Studies on **Th-2,2**. The electrochemistry of **Th-2,2** is similar to that of **Th-3,3**, with the irreversible oxidation of **Th-2,2** occurring at 1.56 V. This derivative has been successfully polymerized, and the voltammetric behavior of the obtained **PTh-2,2** resembles that of **PTh-3,3**, indicating that the different mode of attachment of the thiophene rings in the monomer units does not have a significant effect on the electrochemistry of the resultant polymers. Similar to the observed behavior of **PTh-3,3**, the **PTh-2,2** film exhibited a reversible color change from yellow to black upon oxidation and showed a reproducible electrochemical response when cycled from −1.1 to 2.1 V.

The spectroelectrochemical investigation of **PTh-2,2** was performed by employing a monomer-free electrolyte solution and using the same range of potentials as those applied during the characterization of the film by CV. Figure 6 shows the acquired SNIFTIRS spectra collected at successively higher potentials and normalized to the reference spectrum taken at 0.3 V.

Analysis of the spectra between 800 and 1600 cm^{-1} confirms the presence of the IRAV bands. A very broad absorbance ($\Delta\nu = 2000$ cm^{-1}) attributed to the electronic transition between the valence band and the lowest polaron or bipolaron state is observed at 2500 cm^{-1}. Solvent bands can be seen pointing upward at 2250 cm^{-1} and centered around 3000 cm^{-1}. The incorporation of electrolyte anions (PF_6^-) as a means of maintaining charge neutrality of **PTh-2,2** upon p-doping should give rise to an increasing negative band, as occurred in the case of **PTh-3,3**. Nonetheless, the analysis of the SNIFTIR spectra presented in Figure 7 shows that the band associated with PF_6^- at 845 cm^{-1} is positive, implying a decrease in the anion absorbance when the polymer is being oxidized. Such behavior has been reported for polyaniline[58] and many other polymers[59,60] and can be attributed to the formation of a complex between the PF_6^- and the polymer or PF_6^- and the electrolyte (acetonitrile), which would absorb at a different wavenumber or might also be due to the screening of the absorbance of the PF_6^- anions in that spectral region by the polymer. An increase in the intensity of the SNIFTIR band at 1725 cm^{-1} can also be seen. This peak is, as previously observed for **PTh-3,3**, related to the effect of the doping process on the strength of the C═O bond.

The absence of the C_α-H stretching vibration peak around 3103 cm^{-1} indicates that **Th-2,2** polymerizes via the available α-positions in the thiophene rings. This is in agreement with the higher reactivity of the C_α-H radical in relation to the one formed in the β-position.[7,46] Considering this, the most likely

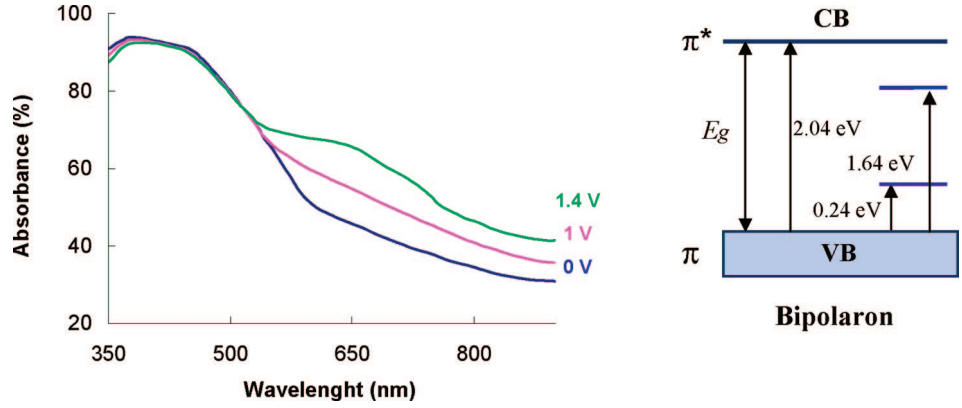

Figure 5. UV−visible spectra of **PTh-3,3** taken at 0, 1, and 1.4 V (left). Band diagram showing the gap state and allowed transitions (CB: conduction band, VB: valence band) (right).

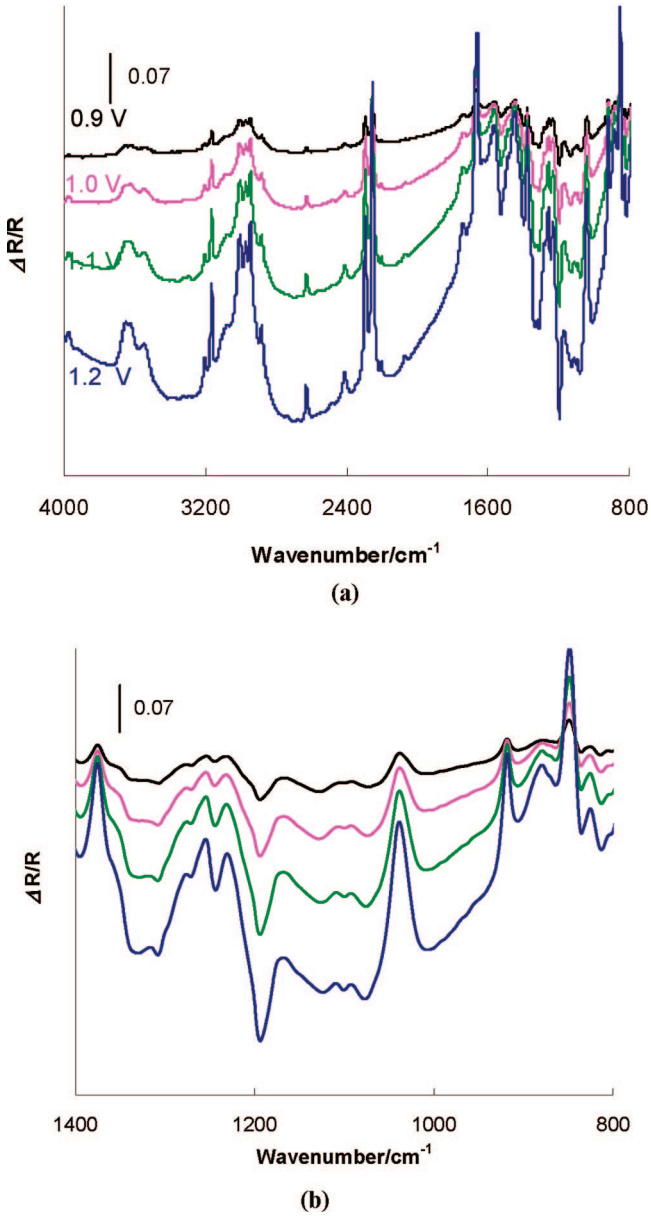

Figure 6. (a) SNIFTIRS spectra of **PTh-2,2** taken from 0.9 to 1.2 V. (b) SNIFTIRS spectra of **PTh-2,2** expansion of region between 800 and 1400 cm^{-1} taken from 0.9 to 1.2 V. Reference spectra collected at 0.3 V.

structure of the polymer formed upon electropolymerization of **Th-2,2** is shown in Figure 7 (top structure).

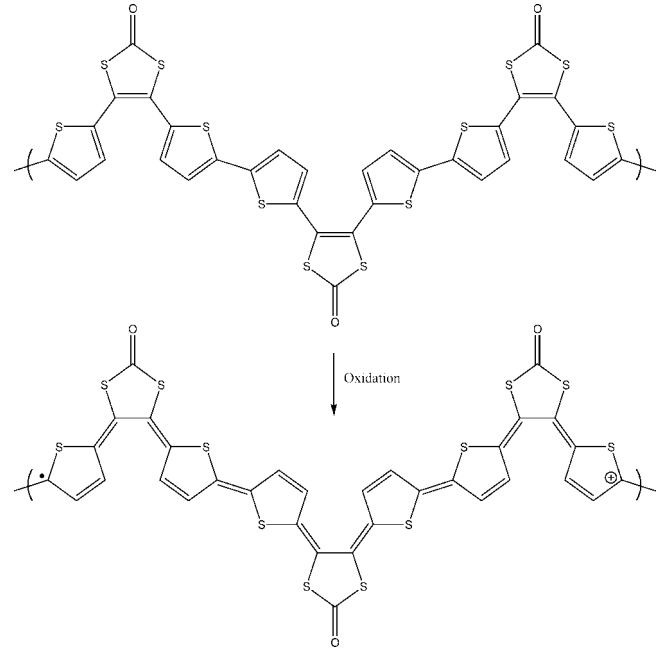

Figure 7. Proposed Structures for **PTh-2,2**.

In-situ UV−visible measurements were carried out on **PTh-2,2** films deposited on an ITO-coated glass working electrode. The films revealed a certain degree of photosensitivity given that a few minutes of exposure to UV−visible radiation would result in loss of electroactivity. Previous reports on the photoreactivity of thiophene 1,3-dithiole-2-ones have shown that the 1,3-dithiole-2-one unit is susceptible to photochemical irradiation, leading to ring cleavage and elimination of carbon monoxide to generate a reactive diradical.[61,62] Given that contrary to the observed response for **PTh-3,3** the electrochemical behavior of **PTh-2,2** is affected by UV−visible radiation, it can be suggested that in this polymer, the 1,3-dithiole-2-ones unit is directly involved in the mobility of charge upon oxidation (Figure 7, lower structure). Consequently, the disruption of the 1,3-dithiole-2-one moiety would reduce the electroactivity of **PTh-2,2**. Because **PTh-3,3** does not appear to show photosensitivity when subject to UV−visible radiation, it can be concluded that the 1,3-dithiole-2-one unit is only partially involved in the conduction mechanism, which would essentially occur through the polythiophene backbone of the polymer. Figure 8 shows the spectra recorded for **PTh-2,2** as the potential was stepped from 0 to 1.2 V.

The UV−visible absorption spectra of **PTh-2,2** at 0 V is characterized by an intense broad absorbance band with a

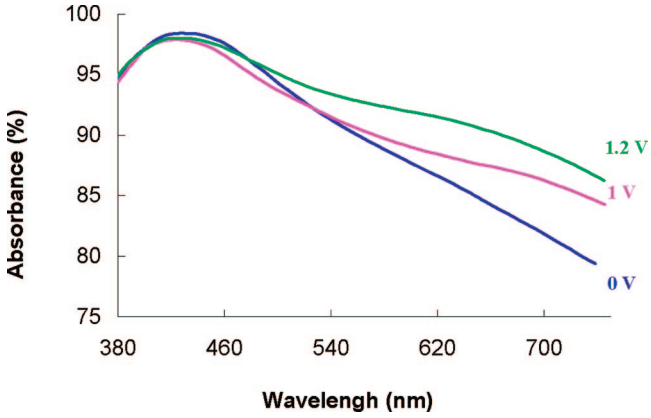

Figure 8. UV−visible spectra of **PTh-2,2** taken at 0 (neutral film), 1, and 1.4 V (doped film).

maximum at 440 nm related to the π-π* transition.[63] The onset of this band is observed at approximately 540 nm, which means that the polymer has a bandgap of 2.3 eV. Upon oxidation, a gradual increase in the absorbance around 650 nm reveals the formation of the charge carrier's typical p-type conducting polymer.[64]

Prompted by electrochemical doping, two new electronic subgap transitions have been identified by UV−visible spectroscopy (Figure 8) and SNIFTIRS (Figure 6). The existence of two midgap transitions is consistent with charge storage, predominantly in bipolarons, as observed in the study of **PTh-3,3**.

Electrochemical and Spectroelectrochemical Studies on **Th-2,3**. Polymerization of **Th-2,3** was achieved by cycling the electrochemical potential up to the irreversible oxidation peak at 1.7 V. The cyclic voltammetry studies on **PTh-3,3** showed a polymer with electrochemical characteristics resembling those of **PTh-3,3** and **PTh-2,2** with the redox switching of **PTh-2,3** being accompanied by a reversible color change from yellow (neutral state) to black (oxidized state). It is clear that all three of the polythiophene 1,3-dithiole-2-ones investigated can be reversibly (and easily) p-doped, yet none of the films undergo n-doping within the potential range studied. We analyzed the stability of **PTh-2,3** by extending the potential limits in the positive and negative directions. The polymer showed a reproducible electrochemical response when cycled from −1.3 to 2.1 V. The SNIFTIRS spectra taken during the stepwise oxidation of **PTh-2,3** are presented in Figure 9.

As the film is oxidized, the distinct bands that are characteristic of conducting polymers are observed: a broadband above 2500 cm^{-1} (onset at 0.23 eV) and several bands in the 1500 to 800 cm^{-1} region. The potential range at which these main spectral changes occur coincides well with the potential where the current peak of the **PTh-2,3** film is observed in the cyclic voltammogram. Once more, the increase in the C═O bond strength upon p-doping is manifested by the shift in the carbonyl group frequency to a higher wavenumber. The development of a sharp peak at 795 cm^{-1} assigned to the C_β-H out-of-plane deformation implies that the bonding between thiophene units occurs mainly through the α-position.

Even though the three polythiophene 1,3-dithiole-2-ones investigated have shown very similar SNIFTIR spectra, the observed subtle differences between them can give insight into their structures. One major distinction lies in the fact that the relative change of reflectance ($\Delta R/R$) in the **PTh-3,3** and **PTh-2,2** spectra (Figures 3 and 6) was found to be about 5 times larger than that for **PTh-2,3** (Figure 11). This different IR behavior seen for the polythiophene 1,3-dithiole-2-ones is clearly illustrated by plotting the change in reflectance of the broadband

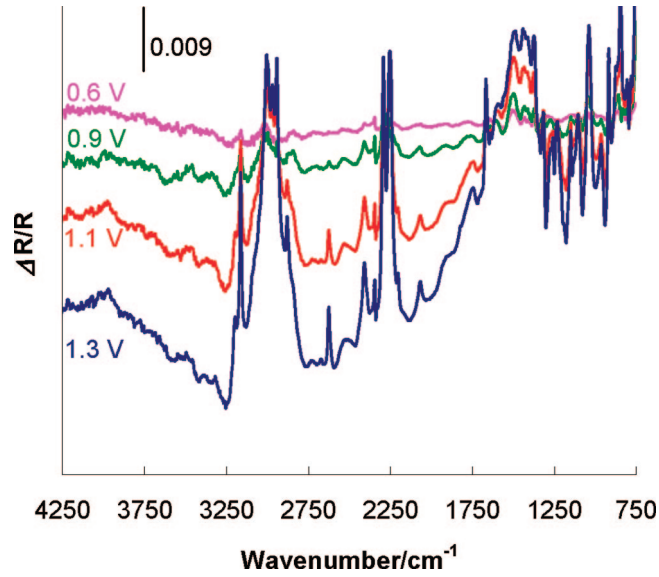

Figure 9. SNIFTIRS spectra of **PTh-2,3** taken from 0.6 to 1.3 V. Reference spectra collected at 0.3 V.

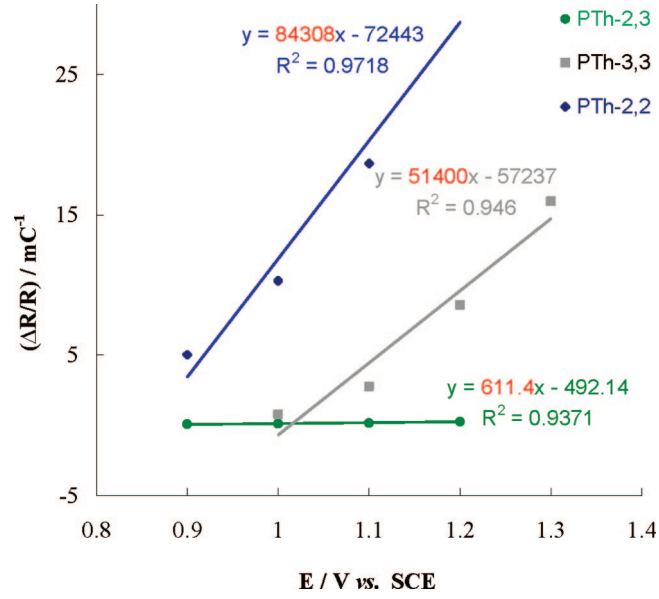

Figure 10. Normalized change in reflectivity as a function of potential for **PTh-2,3**, **PTh-3,3**, and **PTh-2,2**.

centered around 3000 cm^{-1} normalized against charge as a function of the applied potential.

From Figure 10, it can be seen that contrary to the response observed for **PTh-2,3**, the oxidation of **PTh-3,3** and **PTh-2,2** induces a strong increase in the intensity of the IR electronic absorption, prompting a higher slope in the regression curves. One possible explanation is that in these two polymers, and according to their previous suggested structure, all thiophene rings are involved in the movement of electrons. Also, and especially in **PTh-2,2**, there is an important contribution from the 1,3-dithiole-2-one group in the conduction mechanism, leading to increased levels of conductivity. In the case of the monomer **Th-2,3**, polymerization probably occurs via the only thiophene ring with two α-positions available for bonding. Therefore, in the resultant **PTh-2,3** polymer, just a small part of the molecule participates in the transport of charge across the polythiophene backbone. Taking this into account, Figure 11 shows the proposed structure for **PTh-2,3** and the expected quinoid form of this polymer generated upon oxidation.

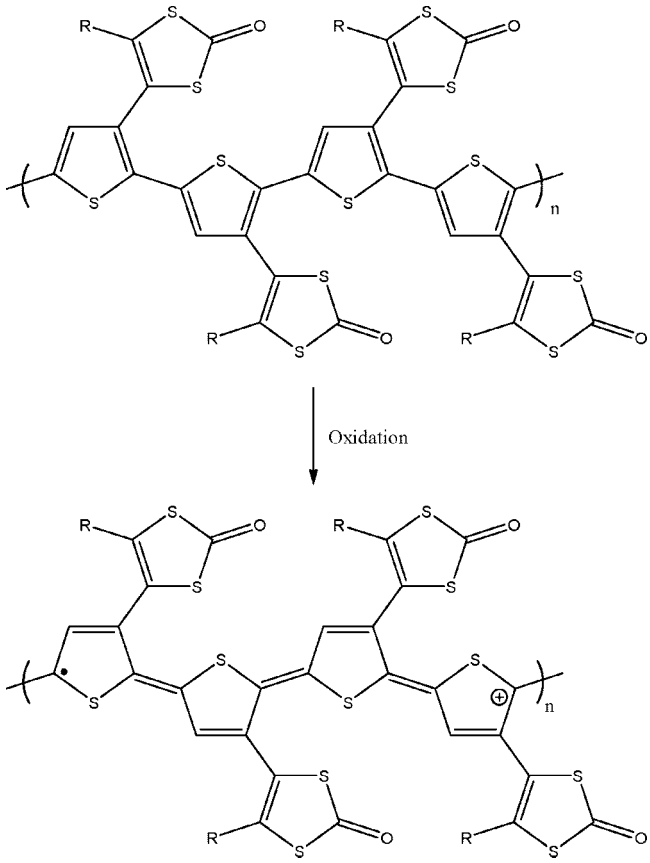

Figure 11. Proposed structure for neutral and oxidized **PTh-2,3** (R = 2-thienyl).

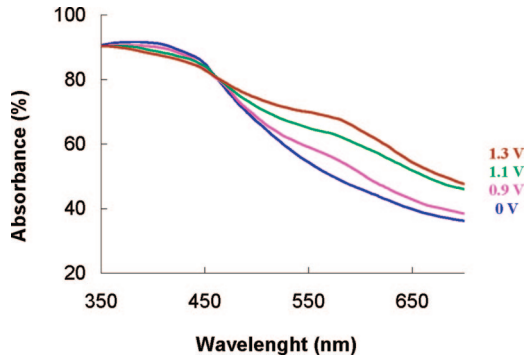

Figure 12. UV−visible spectra of **PTh-2,3** between 0 (neutral film) and 1.3 V (doped film).

The electrochemical switching of **PTh-2,3** between the neutral and oxidized states was investigated by UV−visible spectroscopy. The in situ absorbance spectra recorded at successively higher doping levels are shown in Figure 12.

Contrary to the spectroscopic behavior of **PTh-2,2**, the electroactivity of **PTh-2,3** was not affected by the UV−visible radiation. Because the 1,3-dithiole-2-one group is known to be susceptible to photochemical irradiation, this result confirms the proposed structure of **PTh-2,3**, where the 1,3-dithiole-2-one unit is not directly involved in the movement of electrons (Figure 12).

The analysis of the spectra obtained during the stepwise oxidation of the film in the range of 350 to 700 nm shows a small decrease in the intensity of the broadband centered at 400 nm (assigned to the π-π* transition). The band gap of **PTh-2,3** is estimated to be 2.18 eV from the onset of the absorption of neutral polythiophene. The doping process is accompanied by

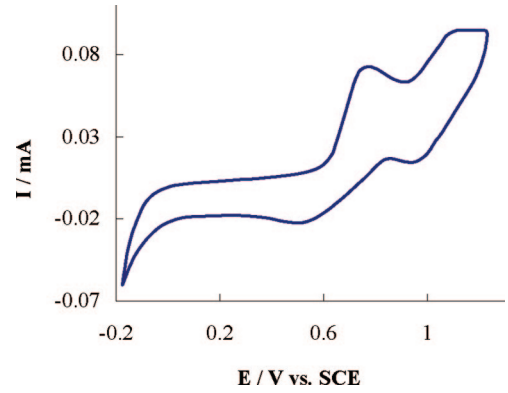

Figure 13. Cyclic voltammogram of **TTF(PTh-3,3)** in monomer-free solution recorded at $v = 0.1$ V s^{-1} using a Pt-disk working electrode (0.44 cm^2).

the appearance of a new broadband at around 585 nm (onset at 1.86 eV), which is characteristic of the presence of free carriers. The presence of an isosbestic point around 525 nm can be interpreted as a two-phase behavior of fully doped and completely undoped chains.[54] In the same way as that suggested by the spectroelectrochemical studies of **PTh-3,3** and **PTh2,2**, the presence of two subgap transitions at 1.86 and 0.23 eV indicates that bipolarons are the charge carriers that are most likely formed upon p-doping of **PTh2,3**.

Electrochemical and Spectroelectrochemical Studies on Th-3,3(2,2′-Me) and Th3,3-(2,5,2′,5′-Me). As previously suggested, the coupling of **Th-3,3**, **Th-2,2** and **Th-2,3** monomer units essentially occurs through the α-position. To confirm this premise, the polymerization of both **Th-3,3(2,2′-Me)** and **Th-3,3-(2,5,2′,5′-Me)**, in which both α-positions are successively blocked, was studied. Polymerization of thiophenes through the β-position has been reported to lead to poor quality films.[46] The electrochemical behavior of **Th-3,3(2,2′-Me)** was investigated by CV. Because the potential was taken above 1.5 V (E_{ox} = 1.67 V), blue-colored species, normally associated with the cation radical of thiophene,[22] could be observed to be streaming away from the electrode surface. Polymerization could only be achieved by prolonged cycling (i.e., 2 h) of the monomer solution between 0.7 and 1.9 V, leading to a poor quality film. Similar experiments on the tetramethylated monomer **Th-3,3(2,2′,5.5′-Me)** demonstrated that this compound also did not undergo polymerization.

Solid-State Chemical in Situ Modification of Thiophene 1,3-Dithiole-2-ones. As discussed earlier, previous studies have shown that the polymerization of thiophene-substituted TTFs was problematic, [24] and to circumvent this, the solid-state modification of the thiophene 1,3-dithiole-2-ones polymers was attempted under Wadsworth−Emmons conditions. Initial efforts to chemically modify the electropolymerized **PTh-3,3**, **PTh-2,2**, and **PTh-2,3** using the phosphonate anion derived from **7**, which had been employed in the synthesis of **8**, proved to be ineffective; however, the ylid **6** proved to be effective.

The electrolyte used during the electropolymerization of thiophenes can have a direct influence on the structure of the obtained films. A different supporting electrolyte (0.1 M of $TBABF_4$ instead of 0.1 M $TBAPF_6$ in acetonitrile) was used during the growth of the thiophene 1,3-dithiole-2-ones. It was envisaged that, as suggested by Marque et al.,[65] the presence of a different anion in the growth electrolyte would affect the morphology and electrochemical properties of the polythiophene 1,3-dithiole-2-one films, enabling their chemical modification. The first outcome of this change in electrolyte was the considerably faster growth of the polythiophene derivatives.

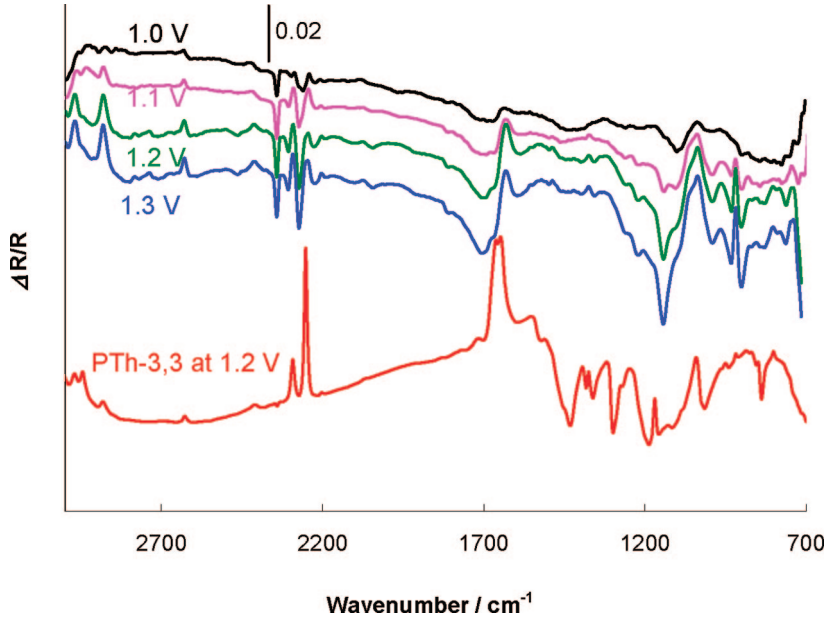

Figure 14. SNIFTIRS spectra of **TTF(PTh-3,3)** taken from 1.0 to 1.3 V. Reference spectra collected at 0.3 V. Spectra were shifted for clarity.

The chemical modification of the electropolymerized polythiophene derivatives was attempted. The Wittig reaction carried out on **PTh-2,3** and **PTh-2,2** was once again ineffective. However, **PTh-3,3** could be successfully modified, and the characteristics of the new polymer were investigated by CV and SNIFTIRS. Figure 13 illustrates the voltammogram of the modified film **TTF(PTh-3,3)**, showing considerable differences in comparison with the CV of the unmodified polymer.

The voltammetric response of **TTF(PTh-3,3)** shows two redox processes ($E^1_{ox} = 0.79$ V/$E^1_{red} = 0.51$ V and $E^2_{ox} = 1.12$ V/$E^2_{red} = 0.95$ V) that are characteristic of TTF redox couples. The calculated half-wave potentials, $E^1_{1/2} = 0.62$ V and $E^2_{1/2} = 1.03$ V, are more positive compared with the standard literature potentials for the TTF unit ($E^1_{1/2} = 0.34$ V and $E^2_{1/2} = 0.71$ V)[66,67] under similar electrochemical conditions. This difference between the half-wave potentials of **TTF(PTh-3,3)** and TTF had been expected because of the introduction of substituents to the TTF unit. The more positive values for the half-wave potentials of **TTF(PTh-3,3)** indicate that this is a relatively less-strong donor system than TTF.

The SNIFTIRS spectra of the **TTF(PTh-3,3)** taken upon stepwise oxidation are shown in Figure 14 alongside with the SNIFTIR spectrum of **PTh-3,3** at 1.2 V.

The spectra reveal an apparent decrease in the conductivity level of **PTh-3,3** upon chemical modification because the shifts observed for doped conducting polymers (IRAVs and broad absorbance band extending into the near IR) are absent in the spectrum of **TTF(PTh-3,3)**. Bands at 763, 827, and 932 cm^{-1} arise from the C−S ring vibrations.[37,68] The positive absorption band at 1040 cm^{-1}, related to the insertion of the $BF4^-$ into the film, is also observed.[36,69] The presence of peaks at 1673 and 1263 cm^{-1}, assigned to the stretching vibration of the C═C bond in TTFs,[70,71] confirms the chemical modification of **PTh-3,3** to **TTF(PTh-3,3)**.

Conclusions

Polythiophene 1,3-dithiole-2-ones have been electrochemically prepared, and their properties have been evaluated by cyclic voltammetry, SNIFTIR, and UV−visible spectroscopy. The voltammetric investigation of **Th-3,3**, **Th-2,2**, and **Th-2,3**, three thiophene 1,3-dithiole-2-ones that differ only in the substitution pattern on the thiophene ring, showed an irreversible oxidation at roughly the same potential for all compounds, owing to the formation of radical cations. The voltammograms of the electrosynthesized polymers were similar and resembled those of many polythiophenes. It was clear that all three polythiophene 1,3-dithiole-2-ones could be reversibly (and easily) p-doped, but none showed stability toward n-doping. They also exhibited an electrochromic effect with the color changing from yellow in the neutral state, to black in the oxidized state.

The spectroelectrochemical investigation of these polymers was performed using the same range of potentials as those applied during the characterization by cyclic voltammetry. The films exhibit IR spectra that are comparable to those of other conducting polymer systems reported in the literature during p-doping. As expected, the spectra were dominated by the appearance of IRAV bands and by a broadband attributed to electronic transitions between the valence band and new subgap states formed upon doping, extending toward the near IR. The SNIFTIRS spectra also revealed the effect of the doping process on the strength of the C═O bond. Upon oxidation, the positive charge on the carbonyl carbon atom increases, which creates a polarized bond, resulting in increased bond strength. This phenomenon was evident in the IR spectra that showed a band associated with the carbonyl group being progressively lost and the peak associated with the oxidized polymer becoming increasingly dominant. The absence of the C_α-H stretching vibration peak was indicative of the presence of α,α-coupling between thiophene rings. Also, the analysis of subtle differences between the SNIFTIR spectra of **PTh-3,3**, **PTh-2,2**, and **PTh-2,3,** specifically, the change in reflectivity upon doping, gave insight into their structures. It is possible that whereas in **PTh-2,2** and **PTh-3,3**, almost all of the molecule can participate in the conduction mechanism, in the case of **PTh-2,3**, only one of the thiophene rings is involved in the transport of charge across the polythiophene backbone.

UV−visible spectroscopy has been used to examine the optical behavior of the polythiophene 1,3-dithiole-2-ones. The UV−visible spectra of the neutral polymers exhibited an absorbance band assigned to the π-π^* transition. From the onset of this transition, it has been determined that **PTh-3,3**, **PTh-2,2**, and **PTh-2,3** have bandgaps of 2.04, 2.30, and 2.18 eV, respectively. Oxidation of the polymer films was accompanied by the appearance of a new broad absorption band characteristic of the presence of free carriers. Because the electrochemical doping of **PTh-3,3**, **PTh-2,2**, and **PTh-2,3** has triggered the

appearance of two new electronic subgap transitions revealed by UV−visible spectroscopy and SNIFTIRS, it has been suggested that bipolarons are the charge carriers that are most likely formed upon p-doping of the polythiophene 1,3-dithiole-2-ones.

The solid-state modification of the synthesized polymers was attempted using standard Wittig conditions. Chemical modification was achieved for **PTh-3,3** but only when using $TBABF_4$ instead of $TBAPF_6$ as the electrolyte salt; however, the voltammetry of the two polymers films was identical. Cyclic voltammetric studies on **TTF(PTh-3,3)** showed the presence of the characteristic TTF redox couples corresponding to the TTF unit of the modified film. SNIFTIRS data also confirmed the presence of the TTF group (C═C vibrations at 1263 and 1668 cm^{-1}).

Experimental Section

Chemicals were obtained from the Aldrich Chemicals Company, Lancaster, or Avocado and were used without further purification. Solvents were dried using the standard conditions detailed in the literature. Proton NMR spectra were recorded in $CDCl_3$ unless otherwise stated and were run on a Bruker AC250 spectrometer at 250 MHz unless otherwise stated. ^{13}C NMR spectra were recorded in $CDCl_3$ unless otherwise stated, run on a Bruker AC250 spectrometer at 62.5 MHz unless otherwise stated, and were all decoupled. J values are given in hertz, and chemical shifts are reported as δ values in relation to tetramethylsilane as internal standard. Infrared spectra were recorded as thin films on a Perkin-Elmer 1600 FT-IR spectrometer with absorption frequencies reported in wavenumbers, ν, and recorded at a resolution of 4 cm^{-1}. Elemental analyses were obtained using a Carlo-Erba model 1106 CHN analyzer. Electron impact (EI) and chemical ionization (CI) were recorded on a VG Masslab model 12/253 spectrometer and on a VG analytical ZAB-E spectrometer at the EPSRC Mass Spectrometry Service Centre in Swansea, MA. measurements are reported in Daltons. All glassware used for synthetic purposes was oven dried (250 °C). Glassware used for electrochemical procedures was left in a H_2SO_4/HNO_3 (1:1 mix) bath for 1 h and rinsed with ultra pure water (Elegastat UHQ). The glassware was then steamed for 10 min and dried in an oven (60 °C). All experiments were conducted under blanket coverage of argon unless otherwise stated. *n*-Butyllithium was titrated against diphenylacteic acid in THF or diethyl ether immediately before use. All yields given along with number of moles refer to the pure isolated compound. The electrolyte tetrabutylammonium tetraflouroborate (TBATFB) was dried in a vacuum oven at 60 °C.

Acknowledgment. We thank the University of Wales Bangor (S.R.-B.) and the ESF (T.A.) for funding and the EPSRC mass spectrometry service at Swansea, MA.

Supporting Information Available: X-ray crystallographic data for **Th-3,3**, **Th-3,3(2,2′-Me)**, **Th-3,3(2,2′,5.5′-Me)**, and **8** and cyclic voltammetry data for **8**. This material is available free of charge via the Internet at http://pubs.acs.org.

References and Notes

(1) Davis, F.; Higson, S. P. J. *Biosens. Bioelectron.* **2005**, *21*, 1–20.
(2) Zarras, P.; Anderson, N.; Webber, C.; Irvin, D. J.; Irvin, D. J.; Guenthner, A.; Stenger-Smith, J. D. *Radiat. Phys. Chem.* **2003**, *68*, 87–394.
(3) Sonmez, G.; Schottland, P.; Zong, K.; Reynolds, J. R. *J. Mater. Chem.* **2001**, *11*, 289–294.
(4) Gerard, M.; Chaubey, A.; Malhotra, B. D. *Biosens. Bioelectron.* **2002**, *17*, 345–359.
(5) Novak, P.; Muller, K.; Santhanam, K. S. V.; Haas, O. *Chem. Rev.* **1997**, *97*, 207–281.
(6) Kumar, D. *Synth. Met.* **2000**, *114*, 369–372.
(7) *Conductive Polymers: Synthesis and Electrical Properties*; Nalwa, H. S., Ed.; Handbook of Organic Conductive Molecules and Polymers, Vol. *2*; Wiley: Chichester, U.K., 1997.
(8) Camurlu, P.; Cirpan, A.; Toppare, L. *Mater. Chem. Phys.* **2005**, *92*, 413–418.
(9) Walsh, C. J.; Sooksimuang, T.; Mandal, B. K. *Macromolecules* **1999**, *32*, 2397–2399.
(10) Garnier, F.; Tourillon, G.; Gazard, M.; Dubios, J. C. *J. Electroanal. Chem.* **1983**, *148*, 299–303.
(11) Bulut, U.; Cirpan, A. *Synth. Met.* **2005**, *148*, 65–69.
(12) Andersson, M. R.; Berggren, M.; Gustafson, G.; Hjertberg, T.; Inganas, O.; Wennerstrom, O. *Synth. Met.* **1995**, *71*, 2183–2184.
(13) Adhikari, B.; Majumdar, S. *Prog. Polym. Sci.* **2004**, *29*, 699–766.
(14) Qi, Z.; Rees, N. G.; Pickup, P. G. *Chem. Mater.* **1996**, *8*, 701–707.
(15) Passos, M. S.; Queiros, M. A.; Le Gall, T.; Ibrahim, S. K.; Pickett, C. J. *J. Electroanal. Chem.* **1997**, *435*, 189–203.
(16) Bryce, M. R.; Chissel, A. D.; Gopal, J.; Parker, D. *Synth. Met.* **1991**, *39*, 397–400.
(17) (a) Thobie-Gautier, C.; Gorgues, A.; Jubault, M.; Roncali, J. *Macromolecules* **1993**, *16*, 4094–4099. (b) Uchida, K.; Masuda, G.; Aoi, Y.; Nakayama, K.; Irie, M. *Chem. Lett.* **1999**, 1071–1072.
(18) Huchet, L.; Akoudad, S.; Roncali, J. *Adv. Mater.* **1998**, *10*, 541–545.
(19) Kanibolotsky, A. L.; Kanibolotskaya, L.; Gordeyev, S.; Skabara, P. J.; McCulloch, I.; Berridge, R.; Lohr, J. E.; Marchioni, F.; Wudl, F. *Org. Lett.* **2007**, *9*, 1601–1604.
(20) Skabara, P. J.; Berridge, R.; McInnes, E. J. L.; West, D. P.; Coles, S. J.; Hursthouse, M. B.; Mullen, K. *J. Mater. Chem.* **2004**, *14*, 1964–1969.
(21) Charlton, A.; Underhill, A. E.; Willimas, G.; Kalaji, M.; Murphy, P. J.; Malik, K. M. A.; Hursthouse, M. B. *J. Org. Chem.* **1997**, *62*, 3098–3102.
(22) Charlton, A.; Kalaji, M.; Murphy, P. J.; Salmaso, S.; Underhill, A. E.; Williams, G.; Hursthouse, M. B.; Malik, K. M. A. *Synth. Met.* **1998**, *95*, 75–78.
(23) Celli, A. M.; Donati, D.; Ponticelli, F. *Org. Lett.* **2001**, *3*, 3573–3574.
(24) Charlton, A.; Underhill, A. E.; Williams, G.; Kalaji, M.; Murphy, P. J. *J. Chem. Soc. Chem. Commun.* **1996**, 2423–2424.
(25) Hibino, S. *J. Org. Chem.* **1984**, *49*, 5006–5008.
(26) Glaze, A. P.; Harris, S. A.; Heller, H. G.; Johncock, W.; Oliver, S. N.; Strydom, P. J.; Whittall, J. *J. Chem. Soc., Perkin Trans. 1* **1985**, 957–962.
(27) Fabre, J. M.; Giral, L.; Gouasmia, A.; Cristau, H. J.; Ribeill, Y. *Bull. Soc. Chim. Fr.* **1987**, 823–826.
(28) Navarro, A.-E.; Moggia, F.; Moustrou, C.; Heynderickx, A.; Fages, F.; Leriche, P.; Brisset, H. *Tetrahedron* **2005**, *61*, 423–428.
(29) Frisch, M. J.; Trucks, G. W.; Schlegel, H. B.; Scuseria, G. E.; Robb, M. A.; Cheeseman, J. R.; Montgomery, Jr., J. A.; Vreven, T.; Kudin, K. N.; Burant, J. C.; Millam, J. M.; Iyengar, S. S.; Tomasi, J.; Barone, V.; Mennucci, B.; Cossi, M.; Scalmani, G.; Rega, N.; Petersson, G. A.; Nakatsuji, H.; Hada, M.; Ehara, M.; Toyota, K.; Fukuda, R.; Hasegawa, J.; Ishida, M.; Nakajima, T.; Honda, Y.; Kitao, O.; Nakai, H.; Klene, M.; Li, X.; Knox, J. E.; Hratchian, H. P.; Cross, J. B.; Adamo, C.; Jaramillo, J.; Gomperts, R.; Stratmann, R. E.; Yazyev, O.; Austin, A. J.; Cammi, R.; Pomelli, C.; Ochterski, J. W.; Ayala, P. Y.; Morokuma, K.; Voth, G. A.; Salvador, P.; Dannenberg, J. J.; Zakrzewski, V. G.; Dapprich, S.; Daniels, A. D.; Strain, M. C.; Farkas, O.; Malick, D. K.; Rabuck, A. D.; Raghavachari, K.; Foresman, J. B.; Ortiz, J. V.; Cui, Q.; Baboul, A. G.; Clifford, S.; Cioslowski, J.; Stefanov, B. B.; Liu, G.; Liashenko, A.; Piskorz, P.; Komaromi, I.; Martin, R.L.; Fox, D. J.; Keith, T.; Al-Laham, M. A.; Peng, C. Y.; Nanayakkara, A.; Challacombe, M.; Gill, P. M. V.; Johnson, B.; Chen, W.; Wong, M. W.; Gonzalez, C.; Pople, J. A., *Gaussian 03*, revision B.04; Gaussian, Inc., Pittsburgh, PA, 2003.
(30) Sankaran, B.; Reynolds, J. R. *Macromolecules* **1997**, *30*, 2582–2588.
(31) Fernandes, M. R.; Garcia, J. R.; Schultz, M. S.; Nart, F. C. *Thin Solid Films* **2005**, *474*, 279–284.
(32) Patil, A.; Heeger, A. J.; Wudl, F. *Chem. Rev.* **1988**, *88*, 183–200.
(33) *Conductive Polymers: Spectroscopy and Physical Properties*; Nalwa, H. S., Ed.; Handbook of Organic Conductive Molecules and Polymers, Vol. *2*; Wiley: Chichester, U.K., 1997.
(34) Ballarin, B.; Costanzo, F.; Mori, F.; Mucci, A.; Pigani, L.; Schenetti, L.; Seeber, R.; Tonelli, D.; Zanardi, C. *Electrochim. Act.* **2001**, *46*, 881–890.
(35) Hotta, S.; Rughooputh, S.; Heeger, A. J.; Wudl, F. *Macromolecules* **1987**, *20*, 212–215.
(36) Kofranek, M.; Kovar, T.; Lischka, H.; Karpfen, A. *J. Molec. Struct.: THEOCHEM* **1992**, *259*, 181–198.
(37) Kvarnstrom, C.; Neugebauer, H.; Blomquist, S.; Ahonen, H. J.; Kankare, J.; Ivaska, A. *Electrochim. Acta* **1999**, *44*, 2739–2750.
(38) Pohjakallio, M.; Sundholm, G.; Talonen, P. *J. Electroanal. Chem.* **1996**, *406*, 165–174.
(39) Ehrendorfer, C.; Karpfen, A.; Bauerle, P.; Neugebauer, H.; Neckel, A. *J. Molec. Struct.* **1993**, *298*, 65–86.
(40) Lopez Navarrete, J. T.; Hernandez, V.; Casado, J.; Favaretto, L.; Distefano, G. *Synth. Met.* **1999**, *101*, 590–591.
(41) Berlin, A.; Zotti, G. *Synth. Met.* **1999**, *106*, 197–201.

(42) Christensen, P. A.; Hamnett, A.; Hillman, A. R.; Swann, M. J.; Higgins, S. J. *J. Chem. Soc., Faraday Trans.* **1992**, *88*, 595–604.
(43) Hayes, W.; Pratt, F. L.; Wong, K. S.; Kaneto, K.; Yoshino, K. *J. Phys. C: Solid State Phys.* **1985**, *18*, L555–L558.
(44) Christensen, P. A.; Hamnett, A.; Read, D. C. *Electrochim. Acta* **1994**, *39*, 187–196.
(45) Tourillon, G.; Garnier, F. *J. Electrochem. Soc.* **1983**, *130*, 2042–2044.
(46) Chan, H. S. O.; Ng, S. C. *Prog. Polym. Sci.* **1998**, *23*, 1167–1231.
(47) Lankinen, E.; Sundholm, G.; Talonen, P.; Laitinen, T.; Saario, T. *J. Electroanal. Chem.* **1998**, *447*, 135–145.
(48) Beyer, R.; Kalaji, M.; Kingscote-Burton, G.; Murphy, P. J.; Pereira, V. M. S. C.; Taylor, D. M.; Williams, G. O. *Synth. Met.* **1998**, *92*, 25–31.
(49) Casado, J.; Katz, H. E.; Hernandez, V.; Lopez Navarrete, J. T. *Vib. Spectrosc.* **2002**, *30*, 175–189.
(50) Skabara, P. J.; Serebryakov, I. M.; Roberts, D. M.; Perepichka, I. F.; Coles, S. J.; Hursthouse, M. B. *J. Org. Chem.* **1999**, *64*, 6418–6424.
(51) Lankinen, E.; Pohjakallio, M.; Sundholm, G.; Talonen, P.; Laitinen, T.; Saario, T. *J. Electroanal. Chem.* **1997**, *437*, 167–174.
(52) Nowak, M. J.; Rughooputh, S. D. D. V.; Hotta, S.; Heeger, A. J. *Macromolecules* **1987**, *20*, 965–968.
(53) Onoda, M.; Iwasa, T.; Kawai, T.; Yoshino, K. *J. Phys. D: Appl. Phys.* **1991**, *24*, 2076–2083.
(54) Havinga, E. E.; Mutsaers, C. M. J. *Chem. Mater.* **1996**, *8*, 769–776.
(55) Dias, B.; Girotto, E.; Matos, R.; Santos, M.; Paoli, M.; Gazotti, W. *J. Braz. Chem. Soc.* **2005**, *16*, 733–738.
(56) Furukawa, Y. *J. Phys. Chem.* **1996**, *100*, 15644–15653.
(57) Carlberg, C.; Chen, X.; Inganas, O. *Solid State Ionics* **1996**, *85*, 73–78.
(58) Jones, V. W.; Kalaji, M. *J. Electroanal. Chem.* **1995**, *395*, 323–326.
(59) Martinez, Y.; Hernandez, R.; Kalaji, M.; Marquez, O. P.; Marquez, J. *J. Electroanal. Chem.* **2004**, *563*, 145–152.
(60) Foley, J.; Korzeniewski, C.; Pons, S. *Can. J. Chem.* **1987**, *66*, 201.
(61) Celli, A. M.; Donati, D.; Ponticelli, F.; Roberts-Bleming, S. J.; Kalaji, M.; Murphy, P. J. *Org. Lett.* **2001**, *3*, 3573–3574.
(62) Roberts-Bleming, S. J.; Davies, G. L.; Kalaji, M.; Murphy, P. J.; Celli, A. M.; Donati, D.; Ponticelli, F. *J. Org. Chem.* **2003**, *68*, 7115–7118.
(63) *Handbook of Conducting Polymers*; Skotheim, T. A., Ed.; Marcel Dekker: New York, 1986; Vol *1*.
(64) Andersson, M. R.; Berggren, M.; Gustafson, G.; Hjertberg, T.; Inganas, O.; Wennerstrom, O. *Synth. Met.* **1995**, *71*, 2183–2184.
(65) Marque, P.; Roncali, J.; Garnier, F. *J. Electroanal. Chem.* **1987**, *218*, 107–118.
(66) Kaufman, F. B.; Schroeder, A. H.; Engler, E. M.; Kramer, S. R.; Chambers, J. Q. *J. Am. Chem. Soc.* **1980**, *102*, 483–488.
(67) Zotti, G.; Zecchin, S.; Schiavon, G.; Berlin, A.; Huchet, L.; Roncali, J. *J. Electroanal. Chem.* **2001**, *504*, 64–70.
(68) Bakhshi, A. K. *Mater. Sci. Eng., C* **1995**, *3*, 249–255.
(69) Gurunathan, K.; Murugan, A. V.; Marimuthu, R.; Mulik, U. P.; Amalnerkar, D. P. *Mater. Chem. Phys.* **1999**, *61*, 173–191.
(70) Bozio, R.; Zanon, I.; Girlando, A.; Pecile, C. *J. Phys. Chem.* **1979**, *71*, 2282–2293.
(71) Meneghetti, M.; Bozio, R.; Zanon, I.; Pecile, C.; Ricotta, C. *J. Phys. Chem.* **1983**, *80*, 6210–6224.

MA802181B